Li, Y. Q., Hu, Z., Fang, X. & Fonseca, J. (2015). Analysis of micro characteristics and influence factors of foundation pit failure. In: K. Soga, K. Kumar, G. Biscontin & M. Kuo (Eds.), Geomechanics from Micro to Macro. (pp. 565-570). London, UK: CRC Press. ISBN 9781138027077

Analysis of micro characteristics and influence factors of foundation pit failure

Y.Q. Li, Z.L. Hu & X. Fang
Department of Civil Engineering, Shanghai University, Shanghai, China

J. Fonseca
Department of Civil Engineering, City University London, London, UK

ABSTRACT: Combined with the design data of an actual foundation pit, PFC (Particle Flow Code) model was developed and micro characteristics such as porosity, displacement vector field and particle rotation were analyzed when a foundation pit with cantilever soldier pile was unstable. The effect of overload, embedded pile depth and the angle of internal friction of soil on instability of the foundation pit were further analyzed. The results indicate that the displacement field under different overload is distinctly different. When piles are shallowly embedded, the foundation pit is apt to be overall unstable and a triangular shaped area of intense shearing and considerable particle rotation appears to form. The soil mass outside the pit compresses at the beginning and subsequently dilates during the failure of the pit. It is shown that factors such as ground overload and the angle of internal friction of soil greatly affect the overturning stability and the slip failure of the foundation pit.

1 INTRODUCTION

In recent years, the increasing construction in urban areas has posed new challenges to foundation pit projects. The shortage of available land and the complexity of urban underground pipeline cause great difficulties to deep pit excavations. Moreover, the instability of foundation excavation not only causes the failure of foundation pit itself, but also leads to incalculable loss of the surrounding environment and underground pipeline.

Without considering the effect caused by seepage and inrush of groundwater, the stability of foundation pit mainly includes overall stability, anti-overturning and anti-sliding of the retaining structure, as well as basal stability against upheaval. However, there are some limitations when the limit equilibrium method and the finite element method are used for investigating the large deformation and failure of foundation pit. With the development of discrete element method (DEM) theory, PFC software (Cundall 1999) not only can effectively solve the mechanical behavior of deformation and damage, but also analyze the internal microscopic physical and mechanical properties of the soil when a pit is unstable. The influence of the micro-structure in shaping the macro-scale response of the soil has been largely reported in the literature (e.g. Fonseca et al 2013). This work provides new insight into the micro-mechanisms at play in the failure of a foundation pit which will help to improve design practices. A PFC numerical model based on an actual foundation pit is established and its microscopic failure mechanism is analyzed and investigated.

2 THE DEVELOPMENT OF THE PFC MODEL FOR A FOUNDATION PIT

2.1 Project overview

A foundation pit with cantilever piles of dimensions 1.0m (diameter) by 15-17m (length) is located on a sandy section of the subway No. 1 Line, Guangzhou, China, and its excavated depth ranges from 6m to 9m for the sections ADK1+344.38 to ADK1+363.94 (Huang & Hui 1997).

Table 1. Physical and mechanical parameters of soil layers.

Soil layer name	Tawny gravelly sand	Grey silty sand	Dark grey silty sand
Natural unit weight (kN/m^3)	17.0	17.6	17.3
Cohesive force (kPa)	2.0	5.0	5.0
Angle of internal friction (^{o})	28.0	28.0	31.0
Compression modulus (MPa)	50	8.19	10.0
Thickness (m)	0.6	2.1	7.0

The soil layers in this section from the ground surface downwards include miscellaneous fill, silt soil, fine silty sand, medium sand, plastic loam, hard plastic loam and highly weathered sandstone. The

upper miscellaneous fill and silt soil have been cleared in advance before the foundation pit was excavated. In this project, three sub-layers of fine silty sand are considered. The physical and mechanical properties of three sub-layer soils are listed in Table 1.

2.2 Geometrical and microscopic parameters of the foundation pit

According to the project mentioned above, half of the foundation pit is considered for this study and for the development of the 2-D PFC numerical model. In the actual project, the excavated depth and width are 6-9m and 15m respectively, the pile depth is 15-17m. Given that the influence scope of excavation is 3-4 times of the excavated depth, the dimensions of the model are 50m (length) by 30m (depth) and the excavated depth and embedded pile depth of model are 6m and 11m respectively, as shown in Figure 1.

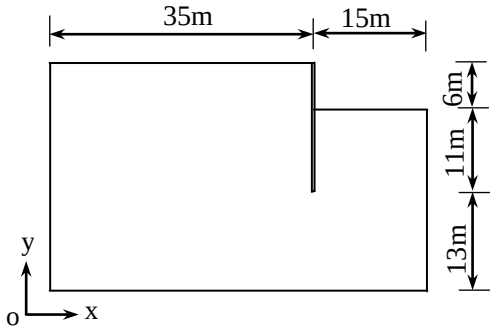

Figure 1. Sketch map of pit model.

Since unit weight, cohesive force and angle of internal friction of three sandy layers involved in foundation pit are similar, homogeneous soil layers are considered in order to simplify the simulation. A slip model is adopted between the soil particles, according to the fitting relationships of sand's macroscopic compression modulus and microscopic normal stiffness, and angle of internal friction and microscopic coefficient of internal friction (Luo 2007). The normal stiffness $k_n=3.75\times10^7$N/m, the shear stiffness $k_s=1.5\times10^7$N/m and the coefficient of friction f=0.7 of sand particles are obtained based on the actual macro physical parameters of soil. The values for the initial porosity and particle density are 0.2 and 1700kg/m^3 respectively.

After the particles are generated by explosive repulsion and looped to the required porosity of 0.2, they are subjected to the sand density and gravity acceleration in order to simulate the settlement process. When either the ratio of maximum unbalanced force of all balls to maximum contact force or the ratio of average unbalanced force to average contact force is less than 1×10^{-4}, it is assumed that the model conforms to the state of the actual deposition process. The height of model is approximately 28.3m after deposition. Considering the arrangement of pile and ground load, the uneven surface part of the model is deleted and the final height is set to 28m.

After the soil deposition, the piling process is simulated using a column with two balls width for a ball diameter of 0.5m and using a contact-stiffness model. The length of pile in the actual project is 17m including 11m embedded length beneath the excavation surface, and the other macro parameters for the pile are shown in Table 2. To avoid the damage caused by insufficient strength of the retaining structure before instability of the foundation pit, a reasonable bond strength for the pile is set. The microscopic parameters used for the pile are shown in Table 3.

Table 2. Macro parameters for the pile.

Radius (m)	Moment of inertia (m^4)	Young's modulus (GPa)	Density ($kg\cdot m^{-3}$)	Shear stiffness (GPa)	Poisson's ratio
0.5	0.04908	28	2500	11.9	0.17

Table 3. Micro parameters for the pile.

Density ($kg\cdot m^{-3}$)	Normal stiffness ($N\cdot m^{-1}$)	Shear stiffness ($N\cdot m^{-1}$)	Normal strength (N)	Shear strength (N)	Coefficient of friction
2500	1.5×10^9	3.0×10^9	2.0×10^{10}	2.0×10^{10}	0.55

The piling method includes deleting the particles at the location of the pile first, followed by embedding pile particles as mentioned above. In order to prevent the overlapping between the soil particles and the pile, the areas to be deleted were slightly enlarged. Once the pile has been defined, the x and y degrees of freedom of the pile are fixed for loop computation, which makes close contact between the pile and the particles around the pile, then these degrees of freedom are freed to go on with the cycle to equilibrium state. The model with the pile in equilibrium is shown in Figure 2. For the convenience of measuring the change of porosity in the process of excavation, the measurement circles are set in the model as shown in Figure 3.

Since the emphasis in this paper is placed on exploring the mechanism of microscopic damage rather than specific values, the radius of particles is magnified. Particle radiuses ranging from 0.090m to 0.099m are chosen for the simulation of the excavation, and the corresponding particle number is

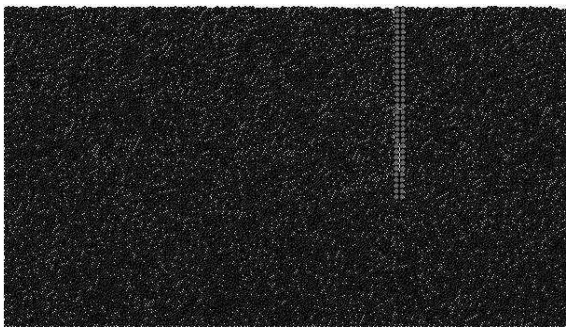

Figure 2. PFC model of piling equilibrium.

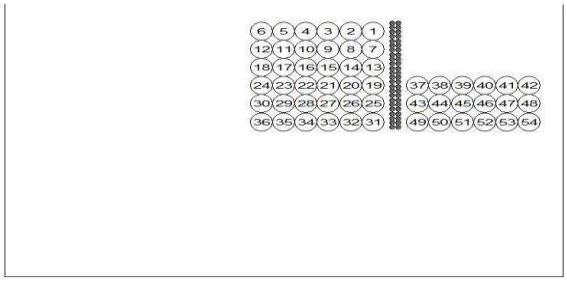

Figure 3. Sketch map of measurement circles location.

42,737. The horizontal displacement measured for the top of the pile in the PFC model is 30.08mm, which is close to the design displacement of 27.65mm.

3 THE EFFECT OF MICROSCOPIC CHARACTERISTICS ON THE FAILURE OF THE FOUNDATION PIT

3.1 Displacement field for different embedded pile depth

A line of particles with an adopted contact-stiffness model, are set for load along x-direction 3m away from the pile in order to investigate the microscopic phenomenon of foundation pit failure with different embedded depth pile. The horizontal (x-direction) freedom of these load particles are fixed to ensure the flexible vertical load. The mean value of ground load is 40kPa. When either the ratio of maximum unbalanced force of all balls to maximum contact force or the ratio of average unbalanced force to average contact force is less than 1×10^{-4}, the loop computation will be interrupted. The model is divided into grilles by soil particles with light color in order that the slip plane outside the foundation pit can be more clearly identified.

The model for a 6m excavated depth and different embedded pile depth is shown in Figure 4 together with the displacement vector fields. A linear slip zone developing from the ground to near the pile bottom can be identified. This triangular shaped zone is more evident for embedded pile depths of 6m and 8m and in these cases the horizontal displacement of the soil is also larger comparing with the other cases. For the pit with 10m and 12m embedded pile depth, the shear zone develops further from the retaining pile. Large settlement values are caused mainly by overall instability of foundation

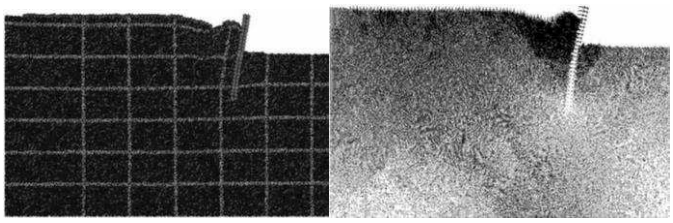
(a). 6m embedded pile depth.

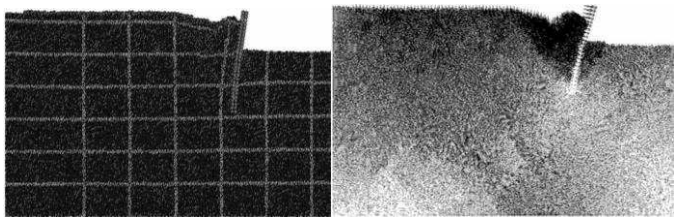
(b). 8m embedded pile depth.

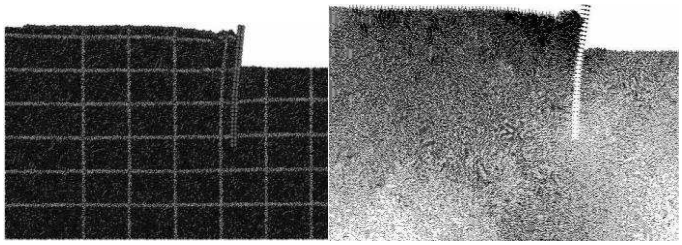
(c). 10m embedded pile depth.

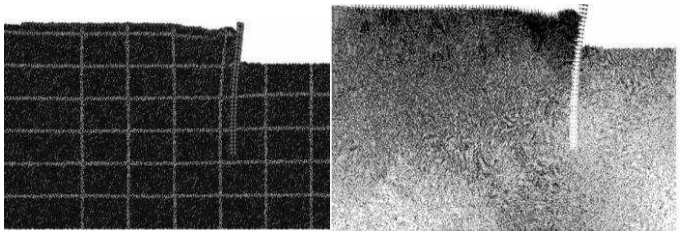
(d). 12m embedded pile depth.

Figure 4. Models with different embedded pile depth and the corresponding displacement vector fields.

pit and the pile rotation around the bottom of the pile. We can observe that for the pits with 6m, 8m and 10m embedded pile depth under 40kPa ground overload outside the pit, the settlement values within the slip surface are much larger comparing with other regions outside the slip surface. Due to the overturning of the retaining pile towards the pit and the pile extrusion influence on the soil near the pile, the displacement field of soil inside the pit follows the same trend and the heave values near the pile are larger than the ones in the middle of the pit.

3.2 Change of porosity in shear zone

The worst case, i.e. the embedded depth of the retaining pile is 6m and the surface overload is 40kpa, is chosen to measure the porosities at the lower part (measurement circle 20), the middle part (measurement circle 15) and the upper part (measurement circle 9) of shear zone outside the pit respectively and the shear zone (measurement circle 38) inside the pit. Variations of the porosities with cycle step are shown in Figure 5.

It can be seen from Figure 5 that the soil outside the pit is under compression state in the early stage, and the porosities decrease gradually. The development of the shear slip surface induces the soil to dilate. The porosities of the lower, middle and upper of shear zone outside the pit and the shear zone inside the pit all increase. The porosity values inside

the pit tend to be significantly higher. Once a stable slip surface forms the porosities tend to a steady value in all the different measured locations.

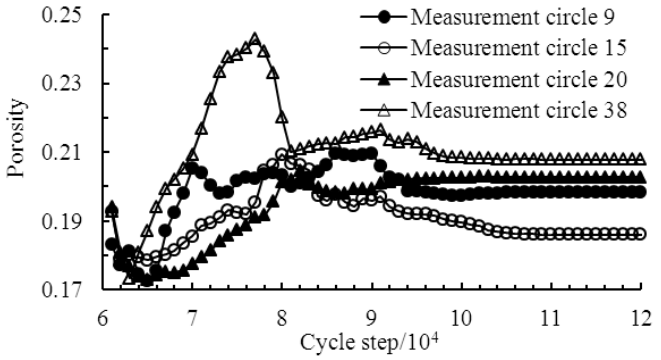

Figure 5. Porosity change for different locations in the shear zone.

3.3 Rotation of particles in the shear zone

Dark color is used to mark the particles with a rotation angle greater than 20° in the process of loop calculation so that they can be identified when the foundation pit is unstable. Figure 6 shows the magnified rotation particles at the area near the pile when the pit is unstable. A considerable number of dark particles can be identified when the pit is unstable for different embedded pile depths. For embedded depths of 6m and 8m the darker particles can be used to identify the triangular shear zone outside the pit. While for embedded depth pile of 10m and 12m the region defined by the dark particles outside the pit is more diffuse, this observation is in accordance with the pattern shown by the displacement vectors in Figure 4. Many particles near the surface rotate due to the downward movement of caused by the loading particles and the horizontal movement of soil particles themselves, while many particles around the retaining pile also rotate because of the vertical movement of the particles, the rotation of the pile and the friction between the soil and the pile.

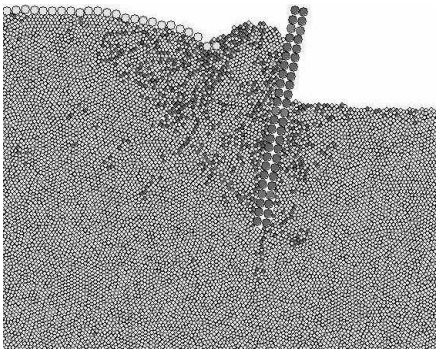

(a). 6m embedded pile depth

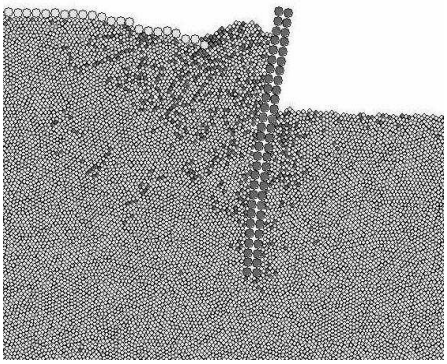

(b). 8m embedded pile depth

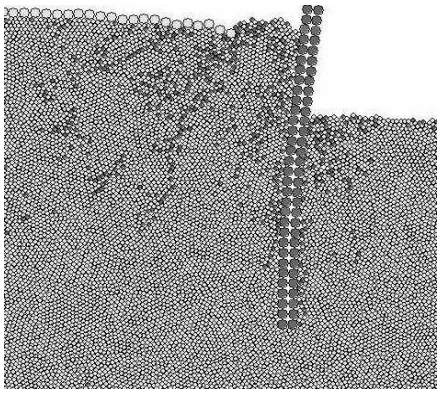

(c). 10m embedded pile depth

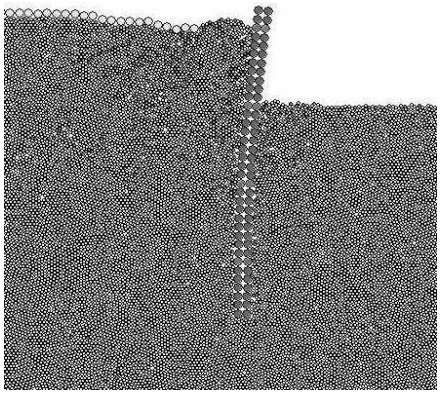

(d). 12m embedded pile depth

Figure 6. Particle rotation models under different embedded depth pile.

4 INFLUENCE FACTORS ON THE FAILURE OF THE FOUNDATION PIT

4.1 Embedded pile depth

The ground settlement curves under different embedded pile depths and for a 40kPa surface overload are displayed in Figure 7. When the embedded depth of the pile is small, the variation in the ground settlement values for different distances from the retaining wall is larger and the maximum settlement value is also larger. However, when the embedded depth of the pile is large (12m embedded depth), the maximum settlement value is small, the curve is smoother and the pit is stable.

4.2 Ground overload

A foundation pit with an excavated depth of 6m and 10m embedded pile depth is used to investigate the influence of the different ground overload of 10kPa,

20kPa, 30kPa and 40kPa. The deformations of the pit are indicated in Figures 8 to 10.

As shown in Figure 8, when there is no overload (0kPa) on the ground surface, the curve is smooth. With the increase of the surface overload, the ground settlement values gradually increase. When the overload is 30kpa and 40kpa, there is sudden change on the ground settlement curves in the range of 3.0m to 5.0m far from the retaining pile, which is regarded as breaking zone of shear region on the ground in the failure of the foundation pit.

According to the horizontal displacement curves for the retaining pile in Figure 9, the curve for the case of no overload does not deviate much from a straight line, however, it is nonlinear under ground overload because of the horizontal displacement and the rotation of pile, and a turning point appears at about 2m depth underneath excavation face (6m). The greater the overload is, the more pronounced the deformation is in terms of translation and rotation of the particles. The horizontal displacements of the top of the pile are respectively 102.2mm and 126.6mm when the overload is 10kPa and 20kPa. However, the same horizontal displacements reach respectively 202.9 mm and 252.0mm when the overload is 30kpa and 40kpa, and the ratios of horizontal displacement to excavation depth reach 3.4% and 4.2% respectively. This is due to the severe overturning of the retaining pile toward the pit, which largely exceeds the specification value (Chang & Zhang 2007). This indicates that the overturning failure of the foundation pit will occur under these conditions.

It can be seen from Figure 10 that the pit base heave becomes larger with the increase of ground overload. The heave values of pit base within the scope of 5m (shear zone) near the retaining pile are larger than for other areas due to the extrusion of the pile. As for the area away from the shear band, the heave is caused mainly by excavation unloading, and it becomes gradually larger from the shear band edge to the center of the pit.

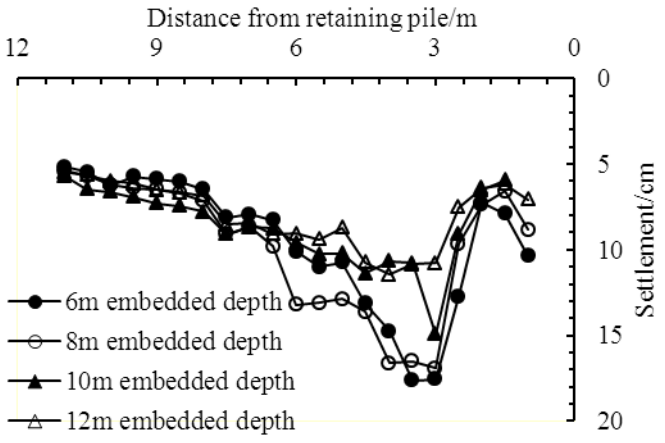

Figure 7. Curves of ground settlement under different embedded pile depth.

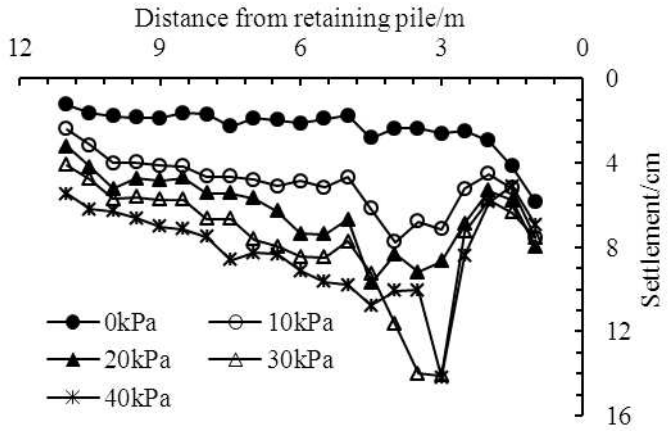

Figure 8. Curves of ground settlement under different overload.

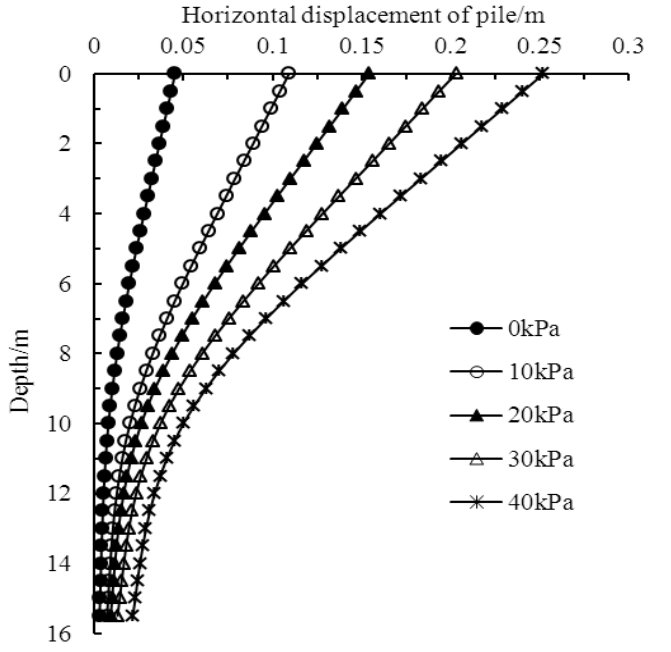

Figure 9. Curves of pile horizontal displacement under different overload.

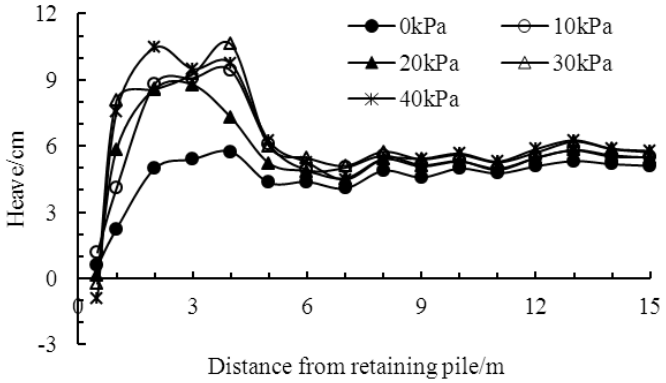

Figure 10. Curves of pit base heave under different overload.

4.3 Angle of internal friction

The angle of friction is an important parameter of shear strength index for soil. From the microscopic point of view, the elastic modulus of particle model without connect is determined by the contact modulus of particles and stiffness ratio, and the strength of model is determined by the coefficient of friction between the particles. The coefficient of friction of the

sandy soil and the corresponding angle of internal friction are presented in Table 4 on the basis of experimental results (Luo 2007). A foundation pit with 10m embedded pile depth and 6m excavated depth under 40kPa overload is modeled and the influence of different coefficient of friction of 0.4, 0.6, 0.8, 1.0 and 1.2 on the horizontal displacement of the pile is shown in Figure 11.

Table 4. Coefficient of friction values and corresponding angle of internal friction values.

Coefficient of friction	0.4	0.6	0.8	1.0	1.2
Angle of internal friction /°	18.8	26.3	33.7	41.2	48.6

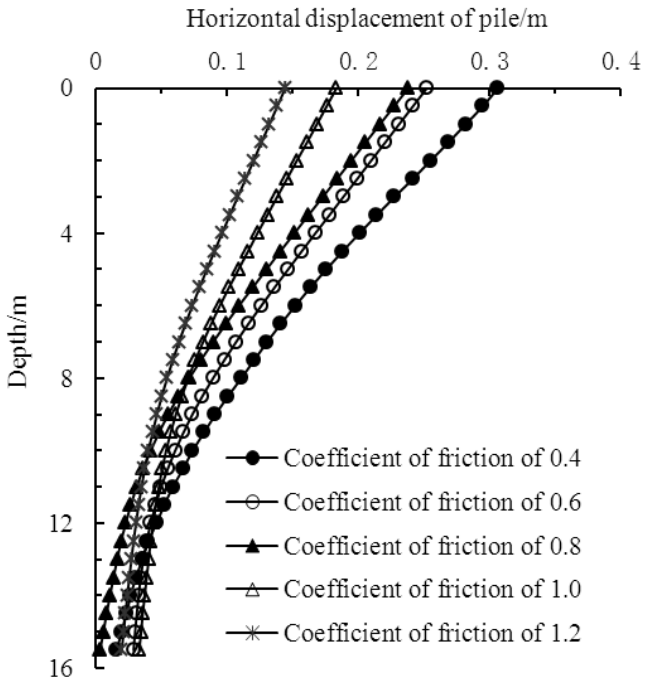

Figure 11. Curves of pile horizontal displacement with different coefficient of friction of a sand.

It can be inferred from Figure 11 that the coefficient of friction of a sand has great influence on the lateral displacement of the foundation pit. The smaller the coefficient of friction, i.e. the smaller the angle of internal friction, the more severe the failure of the supporting structure. When the coefficient of friction is greater than 0.8, it has a marked inhibition effect on the rotation of pile and the horizontal displacement of the top of the pile. For the coefficient of friction of 1.0 and 1.2 decreases about 23.1% and 39.5% compared with the horizontal displacement for the coefficient of friction of 0.8.

5 CONCLUSIONS

Based on an actual sand foundation pit, an analogous PFC numerical model is developed. The microscopic characteristics such as porosity, displacement vector field and rotation of particles are analyzed when the pit is unstable, and the influence of ground overload, embedded pile depth and shear strength of the soil are investigated. This study contributes with important observations on the microscopic mechanisms that lead to instability of a foundation pit and can therefore be used to improve the design and construction of a foundation pit. The conclusions from this investigation can be summarized as follows:

(1) With the decrease of the embedded pile depth, the horizontal displacement of the retaining pile and the heave of pit base increase gradually. The shorter the embedded depth, the more evident the triangular shaped shear zone and the larger the ground settlement in this area of instability. It is demonstrated from the microscopic analysis that by increasing the embedded depth the stability of foundation pit will be improved.

(2) In the initial stage of loading process, porosity of the soil outside the pit decreases due to compression of the soil. The soil porosity in the shear zone increases gradually with the development of the shear zone, which indicates that the shear dilatancy occurs in the process of failure. The porosity values become steady following the complete formation of the shear slip zone. For the shorter embedded pile depth the triangular shaped shear zone is clearly associated with larger values for both the displacement vector field and the particle rotation.

(3) The translation and rotation failures occur firstly in the pit with cantilever pile under different ground overload, the overall failure will happen when load reaches 30kPa. With the increase of the overload, the pit base heave becomes larger.

(4) With the increase of the angle of internal friction of the sand, the horizontal displacement and the rotation of the retaining pile decrease gradually.

ACKNOWLEDGMENT

The investigation was supported by the State Scholarship Fund of China.

REFERENCE

Chang, S. B. & Zhang, S. M. 2007. Engineering geology manual (Fourth Edition). Beijing: China Architecture & Building Press.

Cundall P. A. 1999. *PFC2D user's manual* (Version 3.10). Minnesota: Itasca Consulting Group Inc.

Fonseca, J., O'Sullivan, C., Coop, M. & Lee, P.D. 2013. Quantifying evolution soil fabric during shearing using directional parameters. Géotechnique 63(6): 487-499.

Huang, Q. & Hui, Y. N. 1997. Deep foundation pit engineering instance set. Beijing: China Architecture & Building Press.

Luo, Y. 2007. Simulation of soil mechanical behaviors using discrete element method based on particle flow code and its application. Hangzhou: Zhejiang University.